Supporting Information for "Global impacts from high latitude storms on Titan"

J. Michael Battalio[1]

Juan M. Lora[1]

[1]Department of Earth and Planetary Sciences

Yale University

210 Whitney Ave.

New Haven, CT 06511

Contents of this file

1. Text S1 to S2

2. Figures S1 to S3

Additional Supporting Information (Files uploaded separately)

1. Captions for Movie S1

Text S1: Model description and simulation setup

The Titan Atmospheric Model (TAM; Lora et al., 2015) is a three-dimensional general circulation model of Titan's climate that includes parameterizations for unresolved physics, including a non-gray radiative transfer scheme. TAM self-consistently represents the methane cycle with a hydrology model that allows for surface and sub-surface methane transport (Faulk et al., 2020). The planetary boundary layer is parameterized with a Mellor-Yamada scheme (Mellor & Yamada, 1982). Topography is not directly considered but is a part of the surface hydrology model.

TAM has been validated against a large variety of observations. TAM realistically simulates the temperature, wind and humidity (Lora et al., 2015; Mitchell & Lora, 2016; Lora & Ádámkovics, 2017; Lora et al., 2019), and TAM simulates precipitation and surface liquid patterns that match observations (Faulk et al., 2017; Lora et al., 2019; Faulk et al., 2020; Battalio et al., 2021).

Precipitation occurs via two methods: Large-scale condensation is permitted, but almost all of that falls as virga and re-evaporates before reaching the ground (Battalio et al., 2021). Convection is parameterized using a simplified Betts-Miller scheme (Frierson, 2007; O'Gorman & Schneider, 2008). In the scheme, convection occurs when the convective available potential energy minus the convective inhibition is greater than zero ($CAPE - CIN > 0$). Deep convection occurs when the vertical moisture profile is more moist than a specified reference profile. Shallow convection occurs when the environmental profile is drier than the reference profile. When precipitation occurs, it is immediately placed on the surface. Entrainment is not considered, and the scheme does not change the momentum

fluxes. The scheme's two tunable parameters are the relaxation moisture profile, set to 80%, and the convective timescale, set to 8 hours. Composites were separately tested from simulations varying the relaxation moisture profile between 75% and 85% and the convective timescale between 2 and 8 hours. The results are robust across simulations; thus, we use the optimum parameters (Battalio et al., 2021).

The model setup is identical to that in Faulk et al. (2020) and Battalio et al. (2021). The last year of the model in Battalio et al. (2021) provides the initial conditions for the high temporal resolution run used here. For the compositing methodology, TAM is run at 64 × 32 (lon × lat), with 32 sigma levels for 15 Titan years with output every 2 Titan hours to better resolve the timescales of the higher frequency Rossby waves.

Text S2: Calculation of eddies and heat and momentum spectra

"Eddy" refers to any deviation from zonal-mean quantities. Eddy meridional heat flux spectra are calculated by taking a 2D Fast Fourier Transform of the composited eddy heat flux, v^*T^* at ∼1400 hPa between 41° and 85°N, where v is the meridional wind, T is the temperature, and asterisks denote deviations from the zonal mean. To diagnose waves, spectra are calculated separately over a period of 2–30 Tsols before and after the event in segments 5 Tsols long and averaged.

The idealized dispersion relations shown in Fig. 4a&b are calculated for latitudes of 70° and 85°. The mass-weighted zonal-mean wind and N^2 are calculated over those same latitudes. The average simulated $N^2 \approx 8 \times 10^{-6}$ s^{-2} matches with observations from Huygens (Lorenz et al., 2014). k is calculated for 70° and 85°, and l is assumed to be half

of k. m is calculated assuming the vertical height, H, is 24000 m, taken from Fig. 3, as 400 hPa.

The instantaneous wave phase speed shown in Fig. 4 (blue) is calculated by filtering the eddy surface temperature and eddy surface pressure for zonal wavenumber 1, then tracking maxima in the northern hemisphere and averaging their speeds. The speeds are not substantively different, but averaging does serve to smooth the resulting curve. The idealized Rossby wave phase speed,

$$c_p^x = U - \frac{\beta}{k^2 + l^2 + \gamma^2 + m^2 f_0^2/N^2}, \tag{1}$$

shown in Fig. 4 (orange) is calculated by first finding the mass-weighted vertical-mean zonal wind (U) below 400 hPa over the northern hemisphere. Then, the latitude of the wave maximum is found by following the latitude of the zonal-mean RMS eddy surface pressure maximum filtered for wavenumber 1. The resulting latitudes are used to calculate β and the zonal wavenumber, k. The meridional wavenumber, l, is calculated assuming that the wavelength is twice the distance from the given latitude to the north pole. Times when the northern and southern hemisphere waves are phase locked are defined to have a latitude of 0°, which is determined by finding times when the northern and southern waves have the same sign phase speed in the averaged eddy pressure and temperature fields.

The maximum eddy values in Supplemental Fig. 3 are calculated by searching for the maximum absolute value below 1000 hPa between 8°N/S separately for each variable and plotting the timeseries of that specific latitude, longitude, and pressure.

Movie S1. Movie of the composite evolution of the forced wave in the eddy surface pressure (shading), vertical velocities at 1400 hPa (Pa s^{-1}, contours), and eddy winds at 1400 hPa (vectors) (top); eddy temperatures at 1400 hPa (shading) and eddy moisture at 1400 hPa (contours) (middle); and $CAPE$ (shading) and precipitation (every 5 mm d^{-1}, contours) (bottom).

References

Battalio, J. M., Lora, J. M., Rafkin, S., & Soto, A. (2021). The interaction of deep convection with the general circulation in Titan's atmosphere. Part 2: Impacts on the climate. *Icarus*, 114623. Retrieved from https://doi.org/10.1016/j.icarus.2021.114623 doi: 10.1016/j.icarus.2021.114623

Faulk, S. P., Lora, J. M., Mitchell, J. L., & Milly, P. C. (2020). Titan's climate patterns and surface methane distribution due to the coupling of land hydrology and atmosphere. *Nature Astronomy*, *4*, 390–398. Retrieved from http://dx.doi.org/10.1038/s41550-019-0963-0 doi: 10.1038/s41550-019-0963-0

Faulk, S. P., Mitchell, J. L., Moon, S., & Lora, J. M. (2017). Regional patterns of extreme precipitation on Titan consistent with observed alluvial fan distribution. *Nature Geoscience*, *10*(11), 827–831. doi: 10.1038/NGEO3043

Frierson, D. M. W. (2007). The dynamics of idealized convection schemes and their effect on the zonally averaged tropical circulation. *Journal of the Atmospheric Sciences*, *64*(6), 1959–1974. doi: 10.1175/JAS3935.1

Lora, J. M., & Ádámkovics, M. (2017). The near-surface methane humidity on Titan. *Icarus*, *286*, 270–279. Retrieved from http://dx.doi.org/10.1016/j.icarus.2016.10.012 doi: 10.1016/j.icarus.2016.10.012

Lora, J. M., Lunine, J. I., & Russell, J. L. (2015). GCM simulations of Titan's middle and lower atmosphere and comparison to observations. *Icarus*, *250*, 516–528. Retrieved from http://dx.doi.org/10.1016/j.icarus.2014.12.030 doi: 10.1016/j.icarus.2014.12.030

Lora, J. M., Tokano, T., Vatant d'Ollone, J., Lebonnois, S., & Lorenz, R. D. (2019). A model intercomparison of Titan's climate and low-latitude environment. *Icarus*, *333*(December 2018), 113–126. Retrieved from `https://doi.org/10.1016/j.icarus.2019.05.031` doi: 10.1016/j.icarus.2019.05.031

Lorenz, R. D., Young, L. A., & Ferri, F. (2014). Gravity waves in Titan's lower stratosphere from Huygens probe in situ temperature measurements. *Icarus*, *227*, 49–55. Retrieved from `http://dx.doi.org/10.1016/j.icarus.2013.08.025` doi: 10.1016/j.icarus.2013.08.025

Mellor, G. L., & Yamada, T. (1982). Development of a Turbulence Closure Model for Geophysical Fluid Problems. *Reviews of Geophysics and Space Physics*, *20*(4), 851–875.

Mitchell, J. L., & Lora, J. M. (2016). The Climate of Titan. *Annual Review of Earth and Planetary Sciences*, *44*(1), 353–380. doi: 10.1146/annurev-earth-060115-012428

O'Gorman, P. A., & Schneider, T. (2008). The hydrological cycle over a wide range of climates simulated with an idealized GCM. *Journal of Climate*, *21*(15), 3815–3832. doi: 10.1175/2007JCLI2065.1

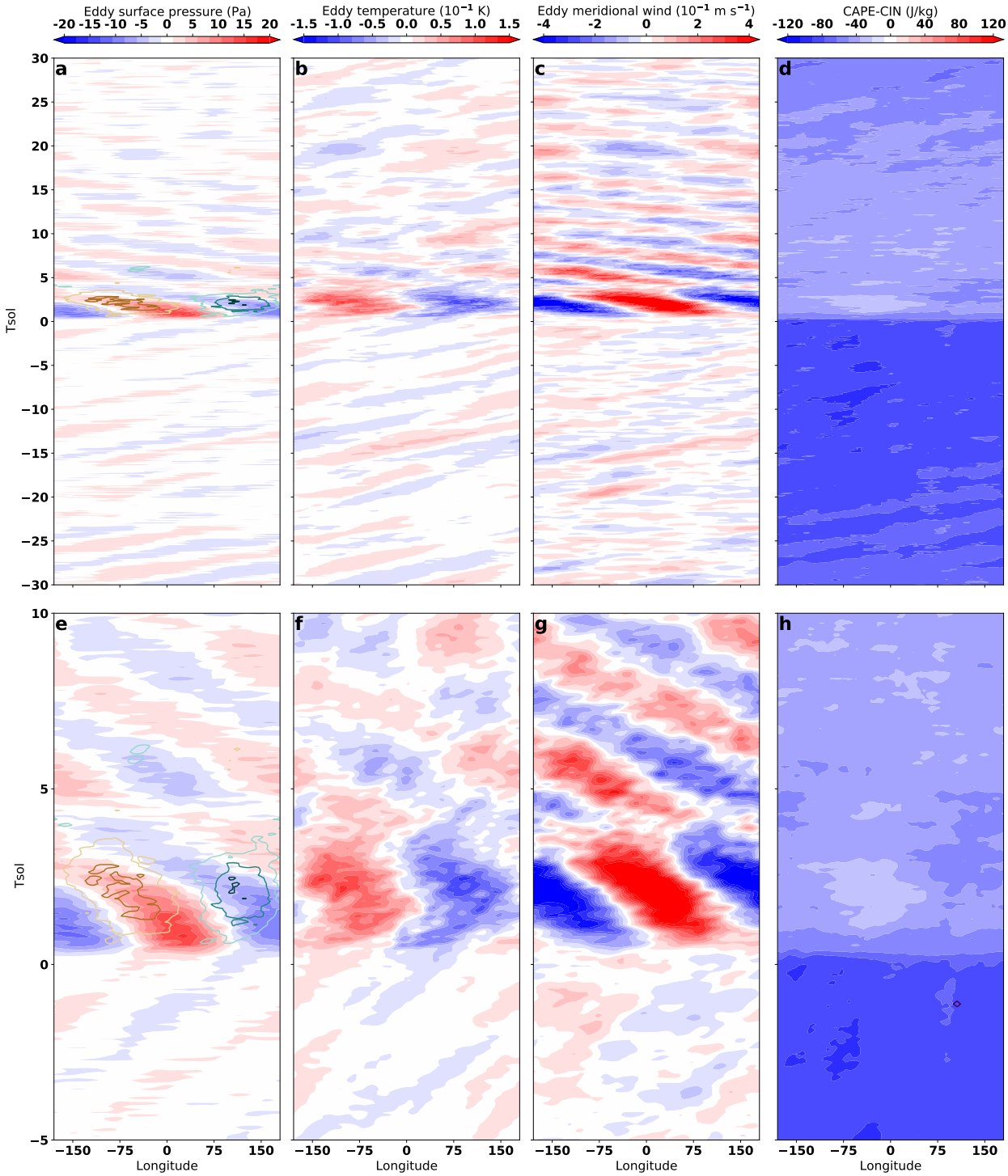

Figure S1. Hovmöller of the same events in Fig. 1 averaged over 41°–85°S. The bottom row repeats the top row over a narrower length of time. Eddy surface pressure (shading) and eddy specific humidity at 1410 hPa (every 10^{-4} g g^{-1} starting at -3, contours) (a, e). Eddy temperature at 1410 hPa (b, f). Eddy meridional wind at 1280 hPa (c, g). $CAPE - CIN$ (d, h).

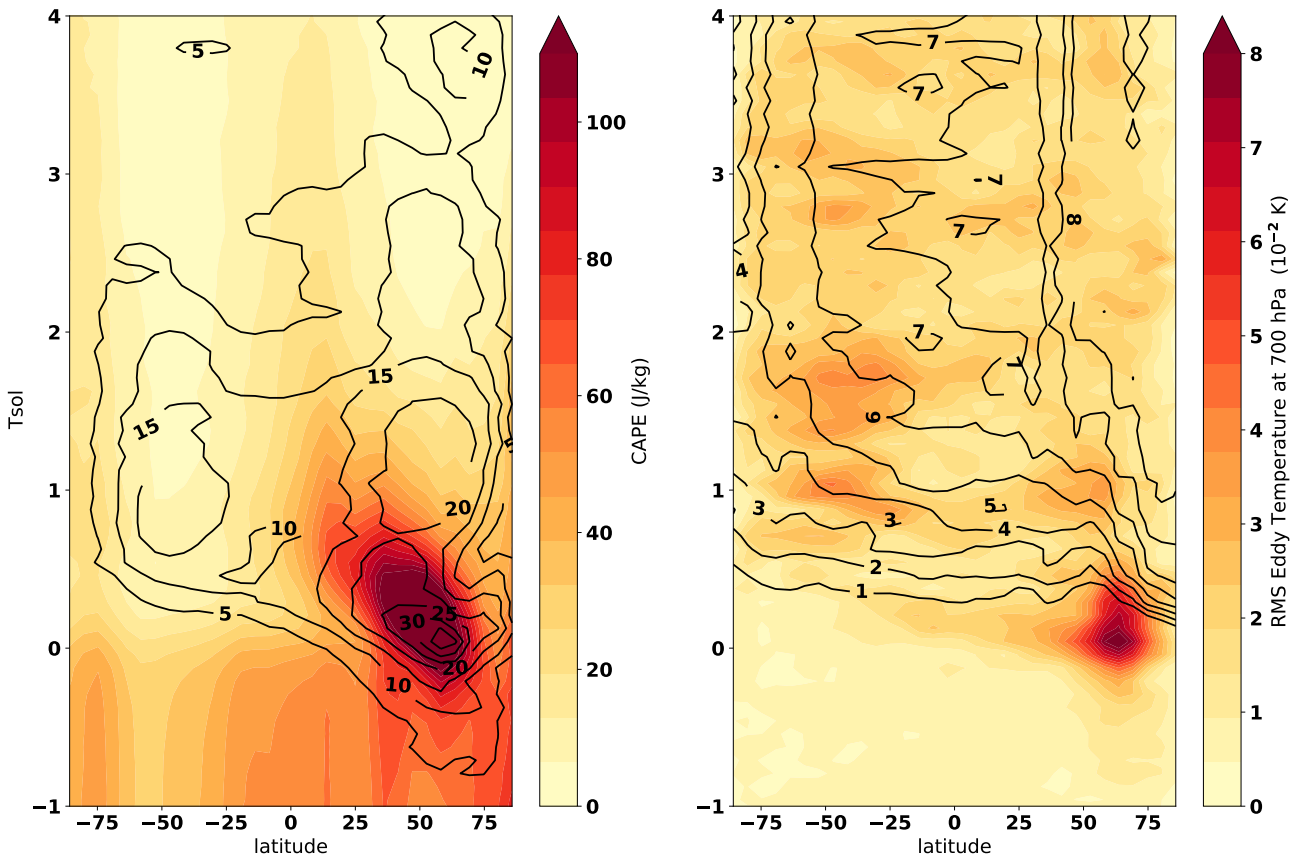

Figure S2. Zonal-mean timeseries of the composited northern hemisphere waves for the $CAPE$ (shading) and RMS eddy surface pressure (contours, Pa) in the left panel and RMS eddy temperature at 700 hPa (shading) and RMS eddy outgoing longwave radiation (contours, 10^{-2} W m^{-2}).

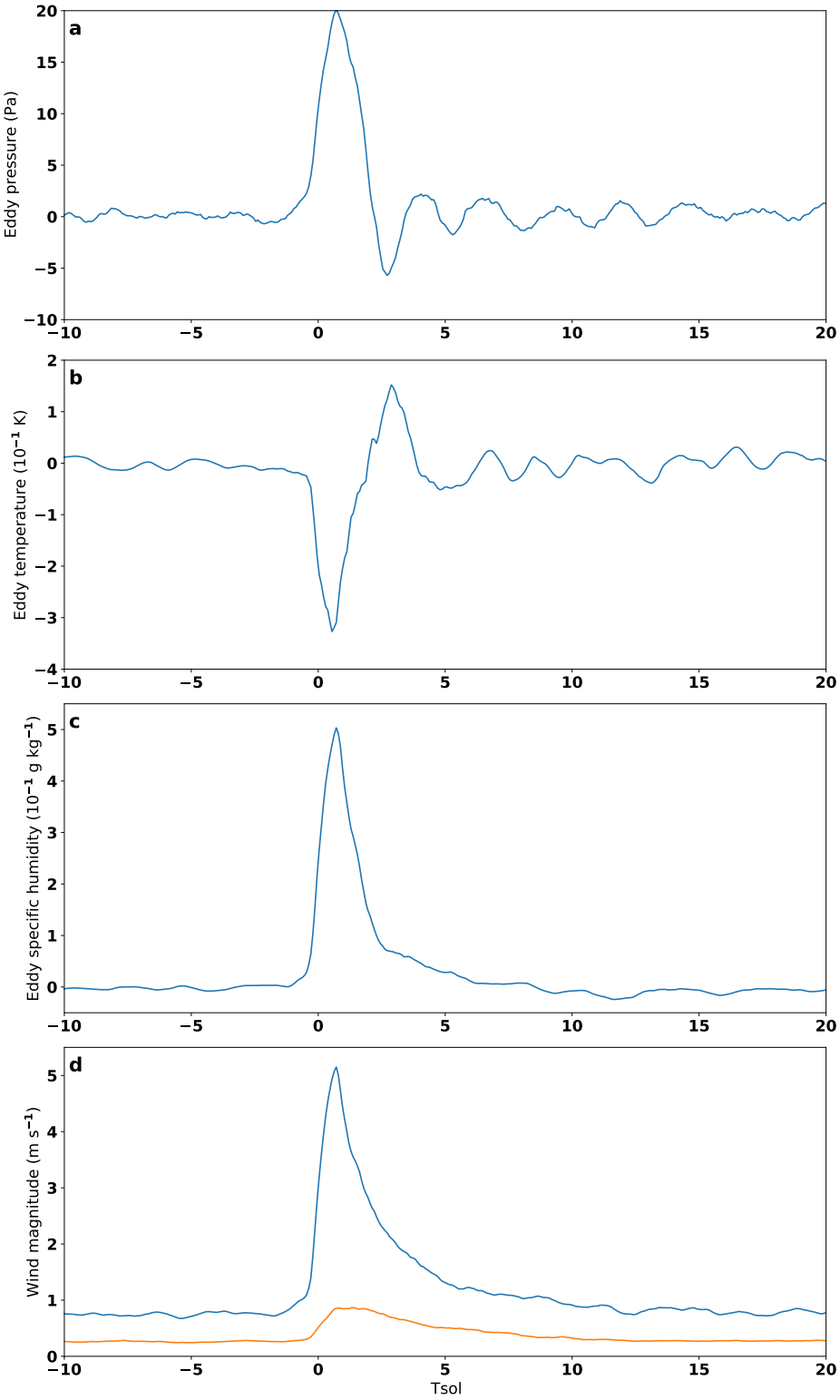

Figure S3. Maximum composite signal at the equator for the eddy surface pressure (a), eddy temperature at 1447 hPa (b), eddy specific humidity (c) and maximum wind magnitude (1447 hPa, blue) and at the surface (orange) (d).